


Article

Effect of Micelle Encapsulation on Toxicity of CdSe/ZnS and Mn-Doped ZnSe Quantum Dots

Qirui Fan ¹, Abhilasha Dehankar ¹, Thomas K. Porter ¹  and Jessica O. Winter ^{1,2,*}

¹ William G. Lowrie Department of Chemical and Biomolecular Engineering, The Ohio State University, 151 W. Woodruff Ave., Columbus, OH 43210, USA; qiruifan1@outlook.com (Q.F.); abhilasha1492@gmail.com (A.D.); tkporter@mit.edu (T.K.P.)

² Department of Biomedical Engineering, The Ohio State University, 151 W. Woodruff Ave., Columbus, OH 43210, USA

* Correspondence: winter.63@osu.edu

Abstract: The optical properties of quantum dots (QD) make them excellent candidates for bioimaging, biosensing, and therapeutic applications. However, conventional QDs are comprised of heavy metals (e.g., cadmium) that pose toxicity challenges in biological systems. Synthesising QDs without heavy metals or introducing thick surface coatings, e.g., by encapsulation in micelles, can reduce toxicity. Here, we examined the toxicity of micelle encapsulated tetrapod-shaped Mn-doped ZnSe QDs, comparing them to 3-mercaptopropionic acid (MPA)-capped Mn-doped ZnSe QDs prepared by ligand exchange and commercial CdSe/ZnS QD systems that were either capped with MPA or encapsulated in micelles. HepG2 cell treatment with MPA-coated CdSe/ZnS QDs resulted in a dose-dependent reduction of viability (MTT assay, treatment at 0–25 µg/mL). Surprisingly, no reactive oxygen species (ROS) or apoptotic signaling was observed, despite evidence of apoptotic behavior in flow cytometry. CdSe/ZnS QD micelles showed minimal toxicity at doses up to 25 µg/mL, suggesting that thicker protective polymer layers reduce cytotoxicity. Despite their shape, neither MPA- nor micelle-coated Mn-doped ZnSe QDs displayed a statistically significant toxicity response over the doses investigated, suggesting these materials as good candidates for bioimaging applications.

Keywords: toxicity; cadmium-free; doped; micelle; quantum dots



Citation: Fan, Q.; Dehankar, A.; Porter, T.K.; Winter, J.O. Effect of Micelle Encapsulation on Toxicity of CdSe/ZnS and Mn-Doped ZnSe Quantum Dots. *Coatings* **2021**, *11*, 895. <https://doi.org/10.3390/coatings11080895>

Academic Editor: Anton Fikai

Received: 30 May 2021

Accepted: 20 July 2021

Published: 26 July 2021

Publisher's Note: MDPI stays neutral with regard to jurisdictional claims in published maps and institutional affiliations.



Copyright: © 2021 by the authors. Licensee MDPI, Basel, Switzerland. This article is an open access article distributed under the terms and conditions of the Creative Commons Attribution (CC BY) license (<https://creativecommons.org/licenses/by/4.0/>).

1. Introduction

Semiconductor nanocrystal quantum dots (QDs) have attracted interest over the past two decades because of their unique opto-electronic properties. QDs have been used in solar cells, light-emitting diodes (LEDs), and lasers, and for bioimaging, biosensing, and therapeutic applications [1–4]. QDs have many advantages compared to their fluorescent molecular dye counterparts for biomedical applications, such as their exceptional brightness, sharp emission peaks, broad excitation spectra, and improved photostability [5]. As a result, QDs are potential alternatives to molecular dyes. However, conventional QDs are synthesised from heavy metal elements, most commonly cadmium, raising concerns about their toxicity in biological systems and the environment [6,7].

Most studies attribute QD toxicity to two main factors: composition and physicochemical properties [8]. As early as 2004 (only 6 years after the first demonstrations of QDs for biological imaging [9,10]), in vitro studies identified toxicity in Cd-based QDs associated with photooxidation and subsequent release of free Cd²⁺ [11]. On the cellular level, cadmium causes DNA damage, elevates reactive oxygen species (ROS) levels that can induce apoptosis, and can be carcinogenic [12]. To address these issues, coatings that improve QD solubility and resistance to photooxidation have been employed (e.g., ZnS shell [6,11], micelle encapsulation [13]). However, QD toxicity is also closely related with cellular uptake [14], which depends on QD physicochemical properties, including QD shape [15]. QDs that enter cells can be more toxic than QDs circulating in the blood or present on the cell

surface [16]. Because QDs are typically manufactured in the organic phase, aqueous phase transfer (e.g., ligand exchange, micelle encapsulation, or silica coating) is often required for biological use. Different transfer strategies produce QDs with different physicochemical properties (e.g., size, surface chemistry, charge) that affect cellular uptake and subsequent subcellular distribution [8,16–19].

Toxicity resulting from composition can be addressed through the use of cadmium-free QDs [20,21]. Several alternative compositions are now available, such as InP- [22,23] and Mn-doped ZnSe- or ZnS-based compositions [24–31]. Mn-doped QDs are particularly interesting because they emit photoluminescence from their doped centres rather than delocalised surface states, increasing photostability against surface chemical- or photo-oxidation [32]. Recently, we reported synthesis of Mn-doped ZnSe QD tetrapods for super-resolution imaging [33]. In this approach, we expanded on a micelle encapsulation aqueous phase transfer method originally introduced by Dubertret [34]. Using block copolymers instead of lipid-polymers to form micelles resulted in enhanced brightness and photostability against high-intensity laser radiation for CdSe/ZnS and Mn-doped ZnSe QDs compared to their unencapsulated counterparts. These improvements were attributed to the thick micelle coating limiting diffusion of oxidative species [33].

However, the effect of the micelle coating on QD toxicity, which is correlated with the presence of oxidative species, was not explored. QDs encapsulated with amphiphilic polymers have been reported to exhibit reduced cellular uptake compared to ligand-coated QDs [13], and toxicity reduction was observed for QDs in several micellar coatings [35–37]. Nonetheless, a generalised claim that micelle coatings outperform ligand exchanged surface coating may be premature. For example, Liu et al. reported that micelle encapsulated QDs showed considerably higher toxicity than their 3-mercaptopropionic acid coated counterparts in neuroblastoma (SH-SY5Y) cell lines [36]. In regard to the Mn-doped QDs, although several toxicity studies have been performed, these studies either used aqueous synthesis methodologies [24,29,30,38–41], or applied the ligand exchange strategy [25,42–44], and none of these QDs adopted a tetrapod morphology.

In this study, we examined the toxicity impact of micelle encapsulation versus ligand exchange on conventional, spherical CdSe/ZnSe QDs and Mn-doped ZnSe tetrapod QDs. For micelle encapsulation, we employed polystyrene-*b*-polyethylene oxide (PS-PEO) block copolymers with -COOH termination, as we employed previously [33]. The PS block forms the hydrophobic core and stabilises the hydrophobic QDs, whereas the PEO block provides water solubility and enhances colloidal stability in the aqueous phase. These materials were selected because of their prior use for nanoparticle encapsulation [45,46] and because of the beneficial biocompatibility properties of PEO [47]. For ligand exchange studies, we evaluated QDs stabilised with 3-mercaptopropionic acid (MPA), as MPA is the most commonly used ligand in the toxicity literature [6,11,14,19,48]. As a model system, we employed HEPG2 human liver carcinoma cell lines, representative of liver cells that would likely be most responsive to heavy metal toxicity. To evaluate toxicity, cell viability and proliferation, ROS generation, and DNA fragmentation were analysed, as these are known toxicity pathways for cadmium-based QDs [49]. These studies provide important information on QD toxicity, including relative contributions from composition versus coating, and provide a path toward synthesising safer QDs for biological use.

2. Materials and Methods

2.1. Materials

Materials for QD synthesis included Zinc stearate (12.5–14% ZnO, Alfa Aesar, Haverhill, MA, USA), Stearic acid (SA, ≥98.5%, Sigma-Aldrich, now MilliporeSigma, St. Louis, MO, USA), selenium powder (99.999%, ~200 mesh, Alfa Aesar), tetramethylammonium hydroxide pentahydrate (TMAH, 25% *w/w* in methanol, Alfa Aesar, Haverhill, MA, USA), manganese chloride (MnCl₂, 97%, Alfa Aesar, Haverhill, MA, USA), 1-octadecene (ODE, ≥95.0%, Sigma Aldrich, St. Louis, MO, USA), octadecylamine (ODA, 98%, Alfa Aesar, Haverhill, MA, USA), and 3-mercaptopropionic acid (MPA, ≥99%, Sigma Aldrich, St.

Louis, MO, USA). Tributyl phosphine (TBP, 97%, Sigma-Aldrich, St. Louis, MO, USA) and acetone ($\geq 99.9\%$, Sigma-Aldrich, St. Louis, MO, USA) were used as solvents. Commercial QDs were used as a comparison were obtained from ThermoFisher (Waltham, MA, USA) in decane (CdSe/ZnS, $\lambda_{em} = 605$ nm) and in pH 9 borate buffer with carboxylic acid termination (CdSe/ZnS, $\lambda_{em} = 605$ nm) [50]. For micelle synthesis, poly(vinyl alcohol) (PVA, 13–23 kDa, 87–89% hydrolysed, Sigma-Aldrich, St. Louis, MO, USA), chloroform (Fisher Scientific, Waltham, MA, USA), and poly(styrene-*b*-ethylene oxide) with a carboxylic acid termination (PS-PEO-COOH) (molecular weight 18-*b*-9.5 kDa, Polymer Source, Dorval, QC, Canada) were employed.

2.2. Preparation of Mn-Doped ZnSe QDs

ZnSe QDs with Mn-doping were prepared according to a previously described procedure [32,51] with modifications [33].

2.2.1. Synthesis of MnSt₂ (Manganese Stearate) Precursor

MnSt₂, used as a precursor for Mn-doping, was synthesised by reacting SA with Mn under basic conditions. First, uniform precipitates of SA were prepared by heating (~50–60 °C) the mixture of SA (1.42 g) and methanol (10 mL) to transparency, followed by cooling the solution until white SA precipitates were observed. The SA precipitates were then dissolved by dropwise addition of TMAH (2.3 mL in 1.5 mL of methanol). Next, MnCl₂ (0.315 g in 3.15 mL of methanol) was added dropwise to the solution above under continuous stirring to induce precipitation of MnSt₂ (white). Lastly, the MnSt₂ precipitate was purified six times by methanol wash (1:15 ratio of solution to methanol) and centrifugal separation recovery (4000 rcf, 10 min), vacuum dried, and stored until use for Mn-ZnSe QD synthesis [50].

2.2.2. Synthesis of Mn-Doped ZnSe QDs

Prior to Mn-doped ZnSe QD synthesis several stock solutions were prepared. A Se stock solution (0.63 g) in TBP (2.7 mL) was made in a glove box. A ZnSt₂ (2.5 g) stock solution was prepared by adding 0.5 g of SA to 12 mL of ODE and heating (~150 °C) the mixture under argon sparging. An ODA (2.5 g)-ODE (2.5 mL) ligand solution was also prepared.

To synthesise QDs, the Se-TBP (1.5 mL) stock solution was injected into a three-neck flask containing 1.3 g of ODA in the glove box. The flask was then removed from the glovebox and rapidly connected to a manifold under argon. The flask was heated to ~70 °C with mild stirring until the ODA dissolved. Meanwhile a separate 100 mL, three-neck reaction flask containing 0.1 g of MnSt₂ and 25 mL of ODE was heated under argon to 110 °C with constant stirring until transparency. The reaction flask was then sparged under argon for an additional 20 min. Following this, the solution was heated slowly to a set point of 290 °C. However, when the solution reached 280 °C, the entire contents of the Se-TBP flask were rapidly injected to the reaction flask. The solution was then brought to 260 °C and held there for an hour.

Next, the reaction temperature was set to 300 °C, and when it reached 290 °C, 4 mL of the ZnSt₂ stock solution at 150 °C was rapidly injected. The solution temperature setpoint was then reduced to 260 °C. Then, the ODA-ODE stock solution was melted with a heat gun under argon and 1 mL was injected into the reaction mixture. Next, three additional injections of 3 mL ZnSt₂ stock solution each were performed every 15 min. Additionally, 1 mL of melted ODA-ODE stock solution was added 5 min after each ZnSt₂ addition. Approximately 15 min after the last injection, the reaction mixture containing Mn-doped ZnSe QDs was cooled to room temperature and stored at 4 °C until purification [50].

2.2.3. Purification of Mn-Doped ZnSe QDs

Purification was performed directly before ligand exchange or micelle encapsulation. First, chloroform (100 μ L) was added to 100 μ L of reaction mixture at 37 °C. The mixture was

heated to 70 °C for complete dissolution and then 200 µL of acetone at room temperature was added to promote flocculation. The final solution was heated again to 70 °C and centrifuged at 20,817 rcf for 20 s to induce pellet formation. Supernatant was discarded, and the pellet was washed twice by repeating this procedure. QDs were then dissolved in chloroform [50]. To confirm QD formation and characterise the product, transmission electron microscopy (TEM) was performed using an FEI Tecnai G2 Spirit TEM (Hillsboro, OR, USA), as well as absorbance and fluorescence measurements using a Thermo Electron Corporation Genesys 6 spectrophotometer (Waltham, MA, USA) and a PTI QuantaMaster™ (Horiba, Kyoto, Japan), respectively. Detailed procedures can be found in Xu, J. et al. [33].

2.3. Preparation of Water-Soluble QDs

2.3.1. Synthesis of MPA-QDs by Ligand Exchange

QDs (commercial CdSe/ZnS or Mn-doped ZnSe) dissolved in chloroform are needed to prepare water-soluble, 3-mercaptopropionic acid (MPA) coated QDs via ligand exchange. As CdSe/ZnS were available in decane, they were transferred to chloroform using a methanol/isopropanol precipitation mixture in a 2:1 volume ratio. As ligands, aliquots of 30 µL MPA were mixed with 300 µL of QDs in chloroform. These solutions were then sonicated for 1 h. Solutions were then centrifuged for purification and washed with an equal volume of chloroform. Further purification was obtained by dissolving the QD pellets in 10 mM NaOH (500 µL) and performing centrifugal filtration (7000 rcf, 3 min each) three times with water using filters with a 100 kDa molecular weight cut-off. QDs were sterilised using 0.22 µm syringe filters and resuspended in cell culture media prior to use [50].

2.3.2. Synthesis of Micelle-Encapsulated QDs

QDs were encapsulated in micelles using the interfacial instability method [52]. Briefly, 100 µL of CdSe/ZnS QDs (0.35 mg/mL) were mixed with 10 µL of PS-PEO-COOH polymers (20 mg/mL) in chloroform. Then, 3 mL of 5 mg/mL PVA in water were added, forming an emulsion. The mixture was homogenised by bath sonication for 60 min, forming small droplets containing chloroform. The mixture was then placed in an aluminium dish and left on a rocker for 15–60 min to evaporate the chloroform. The solution turned transparent when micelles formed. For control experiments, empty micelles were prepared using 100 µL of chloroform instead of QDs.

However, for Mn-doped ZnSe QDs, the procedure differed. Because ODA has low affinity for the QD surface, it was replaced with octanethiol using ligand exchange to improve photostability of the final product. ODA-coated QDs were dissolved in 300 µL of chloroform and mixed with 30 µL of octanethiol. The solution was then sonicated for 60 min to allow for ligand exchange. The thiol-coated QDs (100 µL) were purified using acetone in methanol (60/40 by volume, followed by 50/50 by volume) 500 µL each for two washes. Between washes, pellets were collected by centrifugation at 20,817 rcf, 2 min each. Purified pellets were dissolved in chloroform to assess QD concentration using absorbance at 440 nm (i.e., 1 mg/mL QD displayed an absorbance of 0.127 at 440 nm). Following this ligand exchange protocol, Mn-doped ZnSe QDs were encapsulated in micelles by adding 50 µL of 1.3 mg/mL solution of thiol-coated Mn-doped ZnSe QDs in chloroform to 10 µL of 20 mg/mL PS-PEO-COOH polymers in chloroform. To generate an emulsion, 3 mL of 5 mg/mL PVA in water were then added, and the emulsion sonicated with a probe sonicator for 2 min. As above, this solution was then transferred in an aluminium dish to evaporate the chloroform on a rocker for 15–60 min until micelles formed.

All micelle and QD solutions were sterilised using 0.22 µm syringe filters prior to use. Because of a large excess of PVA, QDs were also washed five times with sterile DI water using centrifugal filtration before suspension in cell culture media [50].

2.4. Toxicity Assays

Toxicity was assessed using a HepG2 liver cell culture model (ATCC, Manassas, VA, USA). Cells were propagated in minimum essential medium (MEM) (Gibco now ThermoFisher, Waltham, MA, USA) with 10% foetal bovine serum (FBS) (Fisher Scientific, Waltham, MA, USA), 1% penicillin/streptomycin (10k U/mL), and 0.2% Mycozap™ (Lonza, Basel, Switzerland) added. Cells were cultured in 5% CO₂ incubators at 37 °C, fed every other day, and passaged at confluency (~80%) [50]. QDs for toxicity assays were diluted using concentrated media which was prepared using 10X MEM solution (97 g/L, 1 mL) (ThermoFisher, Waltham, MA, USA) added to 10X sodium bicarbonate (22 g/L, 1 mL) (ThermoFisher, Waltham, MA, USA), FBS (1 mL), penicillin/streptomycin (0.1 mL), 0.2 mL Mycozap™. This solution was sterilised using a 0.22 µm syringe filter (ThermoFisher, Waltham, MA, USA) prior to use.

2.4.1. MTT Assay

As an initial measure of toxicity, cell metabolism was evaluated with the Vybrant® MTT (3-(4,5-dimethylthiazol-2-yl)-2,5-diphenyltetrazolium bromide) Cell Proliferation Assay Kit (V-13154, Life Technology now ThermoFisher, Waltham, MA, USA). This assay evaluates the enzymatic reduction of MTT by NAD(P)H-dependent cellular oxidoreductase.

Experiments were performed in 96-well plates (5000 cells/well) in replicates of five for each dose. Cells were allowed to propagate for 24 h before QD solutions (50 µL) were introduced at the desired concentration (i.e., 0, 1.56, 3.13, 6.25, 12.5, and 25 µg/mL) in cell culture media. QD or control solutions were incubated with cells for 1 day, after which QD solutions were removed, and phenol red-free culture media (100 µL, ThermoFisher, Waltham, MA, USA) was added. The MTT assay was performed following the manufacturer's instructions by adding MTT solution (10 µL, 12 mM) for 4 h followed by treatment with 10% SDS (sodium dodecyl sulphate). MTT was detected at 570 nm using a VER-SAmx Tunable microplate reader (Molecular Devices Corp., Sunnyvale, CA, USA) against a standard curve [50].

2.4.2. ROS Assay

In addition to the MTT metabolic assay, cell production of reactive oxygen species was assayed using the CellROX® Green Reagent kit (C10444, Life Technologies now ThermoFisher, Waltham, MA, USA). Cells were cultured in well plates at 20,000 cells/well following manufacturer's instructions. Cell culture medium was used to dilute dye solution (previously diluted 20X in PBS) to a concentration of 12.5 µM. This solution was incubated with treatment and control groups for 30 min. No treatment served as a negative control, whereas cells treated with menadione (50 µL, 100 µM in cell culture media) for 1 h served as a positive control. Samples were washed 2X with PBS (100 µL). Then, fluorescence was assessed using a TECAN GENios Pro fluorescence microplate reader (Männedorf, Switzerland) with FITC filters ($\lambda_{\text{ex}} = 485 \text{ nm}$, $\lambda_{\text{em}} = 535 \text{ nm}$).

2.4.3. TUNEL Assay

Next, cellular apoptosis was assessed using a Click-iT® Plus TUNEL kit with Alexa Fluor® 488 (C10617, Life Technologies now ThermoFisher, Waltham, MA, USA) to determine sub-lethal QD exposure effects and also to distinguish apoptotic and necrotic cell death mechanisms. As in ROS experiments, cells were cultured and QDs applied for 24 h with 3 replicates for each concentration. Cells treated for 60 min with DNase (Life Technologies now ThermoFisher, Waltham, MA, USA, 18068-015, 10 units/mL) served as a positive control. Reagents for the TUNEL assay were employed as per manufacturer's instructions. After QD treatment, cells were washed once with PBS, then fixed with 4% paraformaldehyde. Cells were permeabilised with Triton X-100 solution (0.25% in PBS) (Sigma Aldrich, St. Louis, MO, USA), and EdUTP (deoxyuridine triphosphate modified with biorthogonal alkyne moiety) mixed nucleotides were applied with TdT (terminal deoxynucleotidyl transferase). Alexa 488 was then used to label fragmented DNA nicked

ends via copper (I)-catalysed clock chemistry according to manufacturer's protocols. Cells were then visualised with a TECAN GENios Pro fluorescent microplate reader (Männedorf, Switzerland) using FITC filters ($\lambda_{\text{ex}} = 485 \text{ nm}$, $\lambda_{\text{em}} = 535 \text{ nm}$) [50,53].

2.4.4. Live/Dead Analysis via FI Cytometry

For CdSe/ZnS-MPA QDs at the 2 concentrations (6.25 and 25.0 $\mu\text{g/mL}$) with the lowest viability via the MTT assay, we also assessed cell viability using the LIVE/DEAD™ Cell Vitality Assay Kit, C12 Resazurin/SYTOX™ Green (L34951, Invitrogen, now ThermoFisher, Waltham, MA, USA). In these experiments, cells were cultured in 12-well plates (80,000 cells/well) in 3 replicates for each sample. Cells were cultured for 1 day, after which medium was extracted and QD sample solutions or control solutions were added (1 mL). Solutions were incubated for 1 day, and then cells were removed from dishes using TRED (Fisher Scientific, Waltham, MA, USA) and washed with PBS. Cells were re-suspended at 10^6 cells/mL and C12 Resazurin (50 nM) and SYTOX Green (10 nM) reagents applied (15 min, 37 °C). Flow cytometry analysis was performed using a Becton Dickinson FACS Calibur (Franklin Lakes, NJ, USA) with dilution as needed ($\lambda_{\text{ex}} = 488 \text{ nm}$, $\lambda_{\text{em}} = 530$ and 585 nm). C12-resazurin live stain produces red emission in live cells; SYTOX dead stain labels the nucleus of damaged or compromised cells green, indicating cell death or injury. If a cell displayed both labels, it was categorised as injured [50].

2.4.5. Statistical Analysis

QDs at different concentrations within the same material composition treatment groups were compared using one-way ANOVA with p value < 0.05 indicating significance. When a difference was detected, samples were compared to the control using Dunnett's test using a p value of < 0.05 to indicated significance. MTT and ROS experiments employed three plate replicates with five distinct repeats per sample or control per plate. The average of the background (blank) wells was deducted from the average of the measurement values of the five repeats to calculate the background corrected signal. MTT experiments had a negative control (no treatment) only, whereas ROS experiments had negative (no treatment) and positive (menadione) controls. For each plate, background corrected values were normalised to the negative control, and statistical analysis was performed on these values. The deviations of the five replicates in each plate were calculated and pooled across the three plates to determine the standard variance for each sample or control. The TUNEL assay employed a single plate with three measurement replicates. Background signal (blanks) were subtracted for each value, and statistics were assessed for the replicates. Values were normalised to the negative control average [50].

3. Results

3.1. Characterisation of Mn-Doped ZnSe QDs following Phase Transfer

Mn-doped ZnSe QDs offer an alternative to Cd-based QDs with fluorescence originating from dopant levels, rather than surface states. Tetrapod Mn-doped ZnSe QDs were synthesised using a nucleation-doping strategy [33] in the organic phase. As such, it is necessary to transfer these QDs into the aqueous phase for biological use. For aqueous phase transfer, we compared two approaches (Figure 1): ligand exchange using MPA, a commonly employed QD ligand [54,55], and micelle encapsulation using PS-PEO, which has been shown to reduce toxicity [13]. Individual QDs with sizes $< 10 \text{ nm}$ were observed on aqueous transfer by MPA (Figure 1a). Ligand layer thickness for such materials is estimated at $< 0.5 \text{ nm}$, based on monolayer coverage. In contrast, micelle templating resulted in encapsulation of multiple QDs dispersed inside the polymer matrix (Figure 1b). Micelle sizes ranged from 30–50 nm, which is consistent with our prior work [33]. Although QD micelles displayed good stability under normal conditions, aggregation was observed after concentration by high-speed centrifugation (e.g., 20k rcf) or centrifugal filtration (using 100 kDa filters).

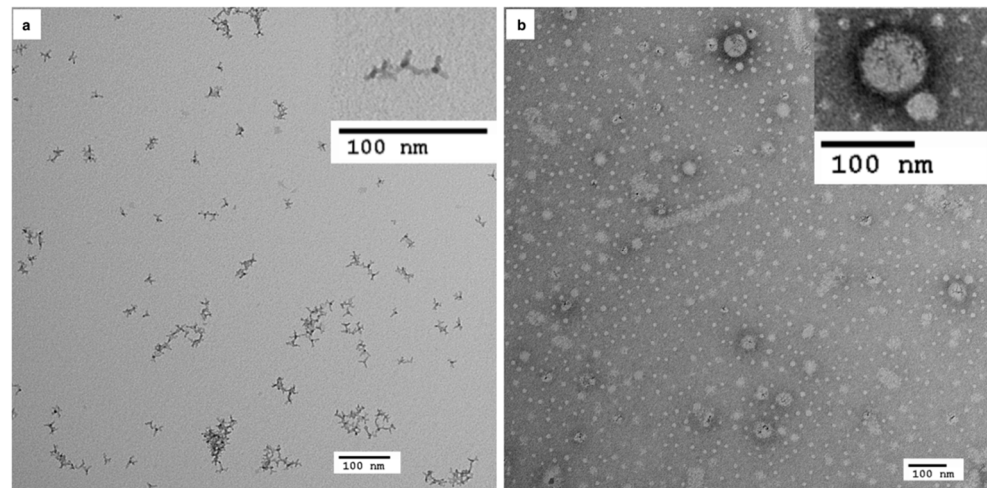


Figure 1. Transmission electron microscopy (TEM) images of (a) MPA-coated and (b) micelle encapsulated Mn-doped ZnSe tetrapod QDs.

3.2. QD Effects on Cell Viability

Initially, cell viability was evaluated using HepG2 cells exposed to MPA-coated and micelle-encapsulated QDs (i.e., CdSe/ZnS and Mn-doped ZnSe) at concentrations ranging from 1.56 to 25.00 $\mu\text{g/mL}$ and compared to untreated controls (Figure 2). Control MPA-coated CdSe/ZnS QDs displayed a statistically significant decrease in viability at concentrations $> 1.56 \mu\text{g/mL}$ with a dose-dependent response (Figure 2a). These results corroborate previous studies of cadmium-based QD toxicity [14,56]. In contrast, MPA-coated Mn-doped ZnSe QDs did not show a statistically significant reduction in cell viability at any concentration tested (Figure 2b). These results are consistent with previous reports of minimal toxicity for Mn-doped QDs [25,27,30]. Despite differences in composition (i.e., ZnSe vs. ZnS or their combination) and synthesis routes, these studies and our work confirm lower toxicity for Mn-doped QDs compared to conventional CdSe/ZnS QDs when ligand exchange is used to form a thin coating on particle surfaces.

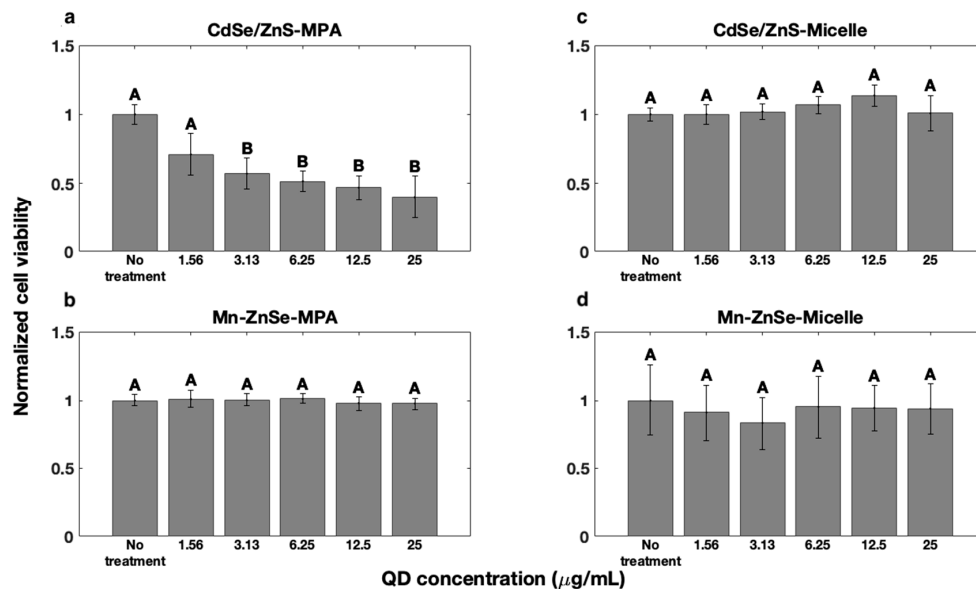


Figure 2. Cytotoxicity of (a,c) CdSe/ZnS and (b,d) Mn-doped ZnSe QDs coated with (a,b) MPA surface ligands or (c,d) encapsulated in PS-PEO polymer micelles as a function of dose as measured by the MTT assay. Bars connected by different letters display statistically significant differences. Thus, bars connected by B are statistically different from controls samples (i.e., samples connected with A).

Next, we evaluated the influence of micelle encapsulation on cell viability. Both CdSe/ZnS and Mn-doped ZnSe QD micelle-encapsulated samples showed no reduction in cell viability over the 24-h incubation used in this study (Figure 2c,d). We also evaluated the potential toxicity of the PVA surfactant used in micelle synthesis and empty micelles (Figures S1 and S2), and observed no statistical difference across the expected dose range.

3.3. Reactive Oxygen Species Formation

Changes in cell viability as measured by the MTT assay reflect the cumulative effects of metabolic rate changes and may result from many factors. Additionally, negligible changes in cell viability may be observed, despite significant changes in other cellular processes. Changes in metabolic rates have been correlated with the presence of oxidative stress in response to ROS [57]. Furthermore, cadmium-based QD cytotoxicity has been associated with the generation of ROS [12]. Thus, we next evaluated ROS levels in cells exposed to QDs. ROS results for cells treated with CdSe/ZnS and Mn-doped ZnSe QDs coated with MPA or encapsulated in micelles were compared to those of untreated cells (Figure 3). Menadione, which stimulates the production of ROS, was employed as a positive control.

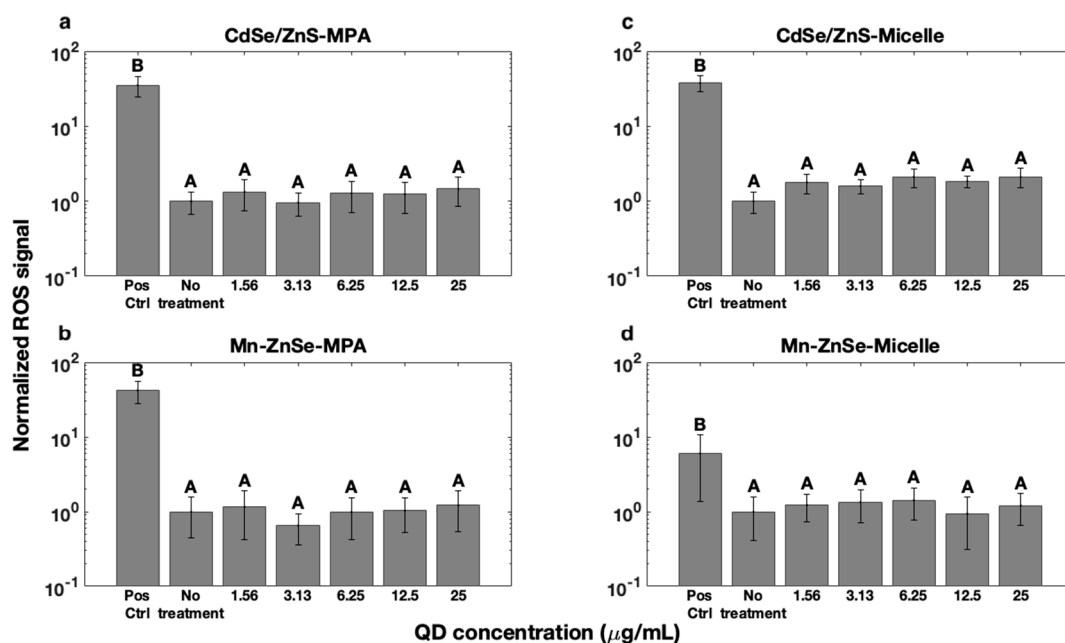


Figure 3. Assessment of ROS production for (a,c) CdSe/ZnS and (b,d) Mn-doped ZnSe QDs (a,b) coated with MPA surface ligands or (c,d) encapsulated in PS-PEO polymer micelles. Results are normalised to no-treatment, negative control groups. Menadione exposure was used as a positive control. Bars connected by different letters display statistically significant differences. Thus, bars connected by A are statistically indistinguishable from negative controls receiving no treatment, and statistically different from positive controls samples exposed to menadione (i.e., samples connected with B).

None of the treatment groups elicited statistically significant increases in ROS production compared to the no treatment controls, nor were dose-dependent trends observed. Similarly, all responses were lower than and statistically different from positive control menadione-treated groups. These results indicate that QD samples did not increase ROS levels in HEPG2 cells at the dosages studied here. Interestingly, ROS generation was not observed for MPA-coated CdSe/ZnS-MPA QD samples (Figure 3a), despite the toxicity observed in the MTT assay (Figure 2a) and previous reports of enhanced ROS production in response to these QDs [58,59]. However, other studies have also reported weak correlation between ROS generation and QD toxicity [19]. For example, ROS-induced QD toxicity can exhibit variable response to ROS inhibitors, with some inhibitors reducing QD toxicity, but others not eliciting an effect [19]. Other work has also shown limited correlation between reduced ROS and increases in cell viability [8], and gene expression analyses

suggest the presence of other toxicity pathways independent of ROS production [8]. Thus, our results suggest that MPA-coated CdSe/ZnS QDs may induce cellular toxicity via an ROS-independent pathway.

3.4. DNA Fragmentation

Since ROS were not observed, we next evaluated DNA fragmentation, a hallmark of apoptosis, using the TUNEL assay. Cadmium has been shown to damage DNA, which may trigger apoptosis [12]. Thus, CdSe/ZnS and Mn-doped ZnSe QDs with MPA coatings and encapsulated in micelles were compared to untreated negative controls and DNase-treated positive controls (Figure 4). No statistically significant differences were detected between samples and untreated control cells, nor were any dose-dependent trends observed. All samples were also statistically different from DNase-treated positive controls. These results indicate negligible change in DNA fragmentation in HEPG2 cells at the dosages studied here. Given the lack of toxicity observed in MTT assays for Mn-doped ZnSe and micelle-encapsulated CdSe/ZnS QDs, this is not surprising and is consistent with other reports [60]. However, CdSe/ZnS QDs capped with MPA did exhibit toxic responses in the MTT assay, and have been reported to elicit DNA damage in the absence of coatings [60]. For these samples, it is possible that the release of cadmium ions was sufficient to impede cell metabolism and proliferation, but not to initiate apoptosis detectable by this assay at this time point.

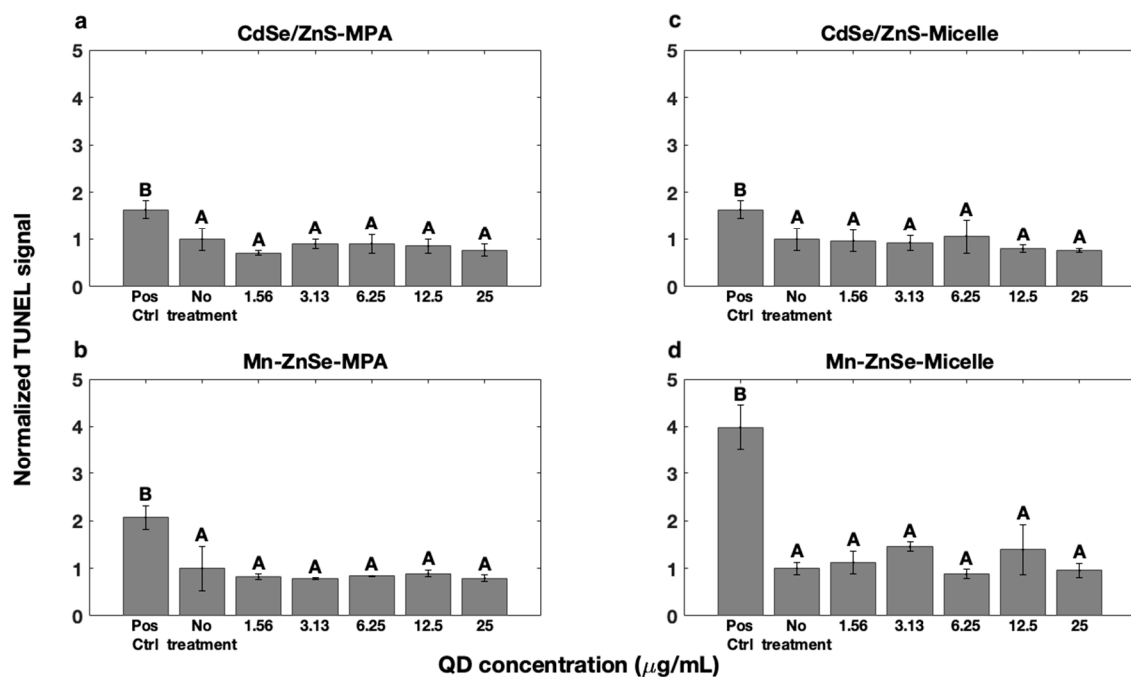


Figure 4. Assessment of DNA fragmentation for (a,c) CdSe/ZnS and (b,d) Mn-doped ZnSe QDs (a,b) coated with MPA surface ligands or (c,d) encapsulated in PS-PEO polymer micelles. DNase exposure provided a positive control. All results are normalised to no-treatment, negative controls. Bars connected by different letters display statistically significant differences. Thus, bars connected by A are statistically indistinguishable from negative controls receiving no treatment, and statistically different from positive controls samples exposed to DNase (i.e., samples connected with B).

To further evaluate this possibility, cell viability in the presence of MPA-CdSe/ZnS QDs was analysed using flow cytometry via a live/dead assay at two concentrations (i.e., 6.25 µg/mL and 25.0 µg/mL) (Table 1). A decrease in the % live cells was observed at the higher 25 µg/mL dose compared to the 6.25 µg/mL dose (78% vs. 83%), with a corresponding increase in the number of injured cells at the higher dose (22% vs. 17%). These data support MTT assay results and suggest that MPA-coated CdSe/ZnS QDs lower metabolic activity because of an increase in the number of injured cells that would most

likely undergo apoptosis over longer time periods. However, further investigation is necessary to determine the cell signalling mechanism(s) responsible for damage after QD treatment.

Table 1. Population Distribution of Cells Assay via a Live/dead Assay in Flow Cytometry in Response to MPA-CdSe/ZnS QD Treatment.

Concentration ($\mu\text{g/mL}$)	Live %	Dead %	Injured %
6.25	82.66	0.19	16.99
25	78.16	0.16	21.64

4. Discussion

This research tested the hypothesis that block copolymer micelle encapsulation of QDs for aqueous stabilisation, which has previously been shown to enhance QD optical properties and photostability, also decreases QD cytotoxicity. Using CdSe/ZnS QDs as a model system, micelle encapsulation clearly showed improved cell viability compared to ligand exchange water solubilisation processes (Figure 2). This was consistent with results from similar phospholipid-PEG micelles that reduce QD toxicity for dosages as high as $\sim 150\text{--}200 \mu\text{g/mL}$ [56]. These results are also consistent with the findings of Smith et al. [13], who found that thicker QD coatings, such as those afforded by block copolymer micelle encapsulation, offer better resistance to oxidation. Previously, we showed that micelle encapsulation protects against high intensity irradiation-induced photobleaching [33], consistent with these findings. Thus, the thick micelle polymer layer employed here may decrease the rate of oxygen diffusion into the micelle, minimising oxidation. Alternatively, lower toxicity may result from preservation of QD crystal structure. In contrast to ligand exchange passivation schemes, micelle encapsulation retains native QD surface ligands (e.g., trioctylphosphine oxide and octadecylamine for CdSe/ZnS and Mn-doped ZnSe QDs, respectively). Ligand exchange processes that displace native organic ligands have been shown to promote the introduction of surface defects by stripping of surface metal cations [61,62]. Thus, micelle encapsulation affords better preservation of the nanocrystal surface, which may reduce susceptibility to oxidative attack.

It is also possible that cell viability observations resulted from differences in cellular uptake efficiency, which is dependent on particle size, shape, and surface charge [18]. Although micelles and MPA-QDs are both negatively charged, micelles ($\sim 30\text{--}40 \text{ nm}$) are much larger than MPA-QDs ($<10 \text{ nm}$), and 50 nm particles. Cellular uptake is optimal for $\sim 50 \text{ nm}$ nanoparticles and those with asymmetric shapes [63]. These attributes suggest that micelles would be more likely to be endocytosed by cells than MPA-QDs. Thus, we conclude that it is unlikely that cellular uptake contributes to reduction in toxicity response, and more likely that improved biocompatibility results from the presence of a thicker diffusive barrier that helps prevent QD oxidation and degradation.

Nonetheless, caution has to be taken when handling these micelles to avoid aggregation, as we observed differences in toxicity for aggregated micelles. In our initial experiments, QD micelles applied at the same concentrations, but prepared from stock solutions of $250 \mu\text{g/mL}$ vs. the $35.0 \mu\text{g/mL}$ employed in this study, elicited toxic responses at concentrations as low as $12.5 \mu\text{g/mL}$ (Figure S3). Both high-speed centrifuge and ultracentrifugation at high concentrations can cause micelle aggregation and irreversible damage to the micelle structure. This likely reduces QD protection against the external environment.

Lastly, we examined the tetrapod shaped Mn-doped QDs, which showed no significant toxicity, either in MPA-coated or micelle-encapsulated forms, at the same concentration as their cadmium-based counterparts. These results are consistent with previous findings in the literature, which used Mn-doped QDs in spherical shape that were prepared either by aqueous synthesis [24,29,30,38–41] or ligand exchange [25,42–44]. The combination of the Mn-doped QDs and the micelle platform may further reduce QD toxicity and provides an attractive candidate for future biological imaging studies.

5. Conclusions

This work examined the cytotoxicity of QDs with two compositions and two surface coatings. Conventional CdSe/ZnS QDs are known to induce cytotoxicity, primarily as a result of Cd²⁺ constituent ions that can be ejected during photo or chemical oxidation [6]. Thus, Mn-doped ZnSe QDs with a tetrapod morphology were examined as an alternative. Mn-doped ZnSe QDs did not elicit statistically significant changes in cell viability, ROS production, or DNA fragmentation regardless of surface coating. Thus, our data support that Mn-doped ZnSe QDs are a promising alternative to more toxic CdSe/ZnS QDs, and that the tetrapod morphology did not negatively impact toxicity. CdSe/ZnS QDs induced cytotoxicity as measured by MTT and live/dead flow cytometry assays [50]. We could not, however, attribute this toxicity response to either ROS production or apoptosis. It is likely that cells were in the early stages of apoptosis, not yet detectable by the TUNEL DNA fragmentation assay. Additional study at longer time points would elucidate this point.

Evaluating the effect of surface coating, thicker micelle coatings have been shown to reduce surface oxidation [13], a likely cause of toxicity. Micelle-templated CdSe/ZnS QDs displayed similar non-toxic behaviour to Mn-doped ZnSe QDs, whereas a concentration-dependent decrease in cell viability was observed for CdSe/ZnS-MPA QDs in both MTT and live/dead flow cytometry assays. These results suggest that our PEG-PEO amphiphilic polymer-based micelle encapsulation processes are more effective at reducing cytotoxic responses to QDs than ligand exchange processes. However, it is not clear if this effect persists at longer time points. Toxicity was observed for QD micelles prepared from more concentrated stock solutions, suggesting aggregation as a potential concern. Additional studies of micelle coating integrity over time and in a wide range of pH and ionic strength conditions would strengthen these conclusions. These data suggest that micelle-templated Mn-doped ZnSe QDs are promising candidates for biological imaging and diagnostic applications with low toxicity and desirable optical properties.

Supplementary Materials: The following are available online at <https://www.mdpi.com/article/10.3390/coatings11080895/s1>, Figure S1: MTT cell viability assay of PVA treated cells as a function of concentration, Figure S2: MTT cell viability assay of empty micelle treated cells at the same concentrations employed in our study, Figure S3: MTT cell viability assay results for cells treated with QD micelles prepared from different concentration stock solutions.

Author Contributions: Conceptualisation, J.O.W. and Q.F.; methodology, J.O.W. and Q.F.; validation, Q.F., A.D. and T.K.P.; formal analysis, A.D. and Q.F.; investigation, Q.F., A.D. and T.K.P.; data curation, Q.F., A.D. and T.K.P.; writing—original draft preparation, Q.F. and A.D.; writing—review and editing, Q.F., A.D., T.K.P. and J.O.W.; supervision, J.O.W.; project administration, J.O.W.; funding acquisition, J.O.W. All authors have read and agreed to the published version of the manuscript.

Funding: This work was funded by the National Science Foundation DBI-1555470 and MCB-1052623.

Institutional Review Board Statement: Not applicable.

Informed Consent Statement: Not applicable.

Data Availability Statement: Data are available upon request from the authors. Please email the corresponding author for access.

Acknowledgments: We thank Yixiao Cui for her assistance with flow cytometry.

Conflicts of Interest: Q.F., A.D. and J.O.W. are currently or have been associated with Core Quantum Technologies (CQT), a company developing QD reagents for research use and clinical diagnostics. CQT provided no support for this work, nor were the materials employed CQT products.

References

1. Carey, G.H.; Abdelhady, A.L.; Ning, Z.; Thon, S.M.; Bakr, O.M.; Sargent, E.H. Colloidal Quantum Dot Solar Cells. *Chem. Rev.* **2015**, *115*, 12732–12763. [[CrossRef](#)] [[PubMed](#)]
2. Shirasaki, Y.; Supran, G.J.; Bawendi, M.G.; Bulovic, V. Emergence of colloidal quantum-dot light-emitting technologies. *Nat. Photon.* **2013**, *7*, 13–23. [[CrossRef](#)]

3. Biju, V. Chemical modifications and bioconjugate reactions of nanomaterials for sensing, imaging, drug delivery and therapy. *Chem. Soc. Rev.* **2014**, *43*, 744–764. [[CrossRef](#)]
4. Hildebrandt, N.; Spillmann, C.M.; Algar, W.R.; Pons, T.; Stewart, M.H.; Oh, E.; Susumu, K.; Diaz, S.A.; Delehanty, J.B.; Medintz, I.L. Energy Transfer with Semiconductor Quantum Dot Bioconjugates: A Versatile Platform for Biosensing, Energy Harvesting, and Other Developing Applications. *Chem. Rev.* **2017**, *117*, 536–711. [[CrossRef](#)]
5. Resch-Genger, U.; Grabolle, M.; Cavaliere-Jaricot, S.; Nitschke, R.; Nann, T. Quantum dots versus organic dyes as fluorescent labels. *Nat. Methods* **2008**, *5*, 763–775. [[CrossRef](#)]
6. Kirchner, C.; Liedl, T.; Kudera, S.; Pellegrino, T.; Munoz Javier, A.; Gaub, H.E.; Stolzle, S.; Fertig, N.; Parak, W.J. Cytotoxicity of colloidal CdSe and CdSe/ZnS nanoparticles. *Nano Lett.* **2005**, *5*, 331–338. [[CrossRef](#)]
7. Hardman, R. A toxicologic review of quantum dots: Toxicity depends on physicochemical and environmental factors. *Environ. Health Perspect.* **2006**, *114*, 165–172. [[CrossRef](#)]
8. Nagy, A.; Steinbrück, A.; Gao, J.; Doggett, N.; Hollingsworth, J.A.; Iyer, R. Comprehensive Analysis of the Effects of CdSe Quantum Dot Size, Surface Charge, and Functionalization on Primary Human Lung Cells. *ACS Nano* **2012**, *6*, 4748–4762. [[CrossRef](#)]
9. Chan, W.C.; Nie, S. Quantum dot bioconjugates for ultrasensitive nonisotopic detection. *Science* **1998**, *281*, 2016–2018. [[CrossRef](#)] [[PubMed](#)]
10. Bruchez, M., Jr.; Moronne, M.; Gin, P.; Weiss, S.; Alivisatos, A.P. Semiconductor nanocrystals as fluorescent biological labels. *Science* **1998**, *281*, 2013–2016. [[CrossRef](#)] [[PubMed](#)]
11. Derfus, A.M.; Chan, W.C.W.; Bhatia, S.N. Probing the cytotoxicity of semiconductor quantum dots. *Nano Lett.* **2004**, *4*, 11–18. [[CrossRef](#)] [[PubMed](#)]
12. Rani, A.; Kumar, A.; Lal, A.; Pant, M. Cellular mechanisms of cadmium-induced toxicity: A review. *Int. J. Environ. Health Res.* **2014**, *24*, 378–399. [[CrossRef](#)] [[PubMed](#)]
13. Smith, A.M.; Duan, H.W.; Rhyner, M.N.; Ruan, G.; Nie, S.M. A systematic examination of surface coatings on the optical and chemical properties of semiconductor quantum dots. *Phys. Chem. Chem. Phys.* **2006**, *8*, 3895–3903. [[CrossRef](#)]
14. Chen, N.; He, Y.; Su, Y.Y.; Li, X.M.; Huang, Q.; Wang, H.F.; Zhang, X.Z.; Tai, R.Z.; Fan, C.H. The cytotoxicity of cadmium-based quantum dots. *Biomaterials* **2012**, *33*, 1238–1244. [[CrossRef](#)] [[PubMed](#)]
15. Sukhanova, A.; Bozrova, S.; Sokolov, P.; Berestovoy, M.; Karaulov, A.; Nabiev, I. Dependence of Nanoparticle Toxicity on Their Physical and Chemical Properties. *Nanoscale Res. Lett.* **2018**, *13*, 44. [[CrossRef](#)]
16. Chang, E.; Thekkekk, N.; Yu, W.W.; Colvin, V.L.; Drezek, R. Evaluation of quantum dot cytotoxicity based on intracellular uptake. *Small* **2006**, *2*, 1412–1417. [[CrossRef](#)]
17. Clift, M.J.D.; Rothen-Rutishauser, B.; Brown, D.M.; Duffin, R.; Donaldson, K.; Proudfoot, L.; Guy, K.; Stone, V. The impact of different nanoparticle surface chemistry and size on uptake and toxicity in a murine macrophage cell line. *Toxicol. Appl. Pharmacol.* **2008**, *232*, 418–427. [[CrossRef](#)]
18. Peng, L.; He, M.; Chen, B.B.; Wu, Q.M.; Zhang, Z.L.; Pang, D.W.; Zhu, Y.; Hu, B. Cellular uptake, elimination and toxicity of CdSe/ZnS quantum dots in HepG2 cells. *Biomaterials* **2013**, *34*, 9545–9558. [[CrossRef](#)]
19. Lovric, J.; Bazzi, H.S.; Cuie, Y.; Fortin, G.R.; Winnik, F.M.; Maysinger, D. Differences in subcellular distribution and toxicity of green and red emitting CdTe quantum dots. *J. Mol. Med.* **2005**, *83*, 377–385. [[CrossRef](#)]
20. Pelley, J.L.; Daar, A.S.; Saner, M.A. State of Academic Knowledge on Toxicity and Biological Fate of Quantum Dots. *Toxicol. Sci.* **2009**, *112*, 276–296. [[CrossRef](#)]
21. Rocha, T.L.; Mestre, N.C.; Saboia-Morais, S.M.T.; Bebianno, M.J. Environmental behaviour and ecotoxicity of quantum dots at various trophic levels: A review. *Environ. Int.* **2017**, *98*, 1–17. [[CrossRef](#)]
22. Brunetti, V.; Chibli, H.; Fiammengio, R.; Galeone, A.; Malvindi, M.A.; Vecchio, G.; Cingolani, R.; Nadeau, J.L.; Pompa, P.P. InP/ZnS as a safer alternative to CdSe/ZnS core/shell quantum dots: In vitro and in vivo toxicity assessment. *Nanoscale* **2013**, *5*, 307–317. [[CrossRef](#)]
23. Lin, G.M.; Ouyang, Q.L.; Hu, R.; Ding, Z.C.; Tian, J.L.; Yin, F.; Xu, G.X.; Chen, Q.; Wang, X.M.; Yong, K.T. In vivo toxicity assessment of non-cadmium quantum dots in BALB/c mice. *Nanomed. Nanotechnol. Biol. Med.* **2015**, *11*, 341–350. [[CrossRef](#)]
24. Liu, J.A.; Wei, X.L.; Qu, Y.; Cao, J.H.; Chen, C.S.; Jiang, H. Aqueous synthesis and bio-imaging application of highly luminescent and low cytotoxicity Mn²⁺-doped ZnSe nanocrystals. *Mater. Lett.* **2011**, *65*, 2139–2141. [[CrossRef](#)]
25. Zhou, R.H.; Li, M.; Wang, S.L.; Wu, P.; Wu, L.; Hou, X.D. Low-toxic Mn-doped ZnSe@ZnS quantum dots conjugated with nano-hydroxyapatite for cell imaging. *Nanoscale* **2014**, *6*, 14319–14325. [[CrossRef](#)]
26. Plumley, J.B.; Akins, B.A.; Alas, G.J.; Fetrow, M.E.; Nguyen, J.; Jain, P.; Yang, S.; Brandt, Y.I.; Smolyakov, G.A.; Ornatowski, W.; et al. Non-cytotoxic Mn-doped ZnSe/ZnS quantum dots for biomedical applications. In Proceedings of the Conference on Colloidal Nanoparticles for Biomedical Applications IX, San Francisco, CA, USA, 1–4 February 2014.
27. Drobintseva, A.O.; Matyushkin, L.B.; Aleksandrova, O.A.; Drobintsev, P.D.; Kvetnoy, I.M.; Mazing, D.S.; Moshnikov, V.A.; Polyakova, V.O.; Musikhin, S.F. Colloidal CdSe and ZnSe/Mn quantum dots: Their cytotoxicity and effects on cell morphology. *St. Petersburg Polytech. Univ. J. Phys. Math.* **2015**, *1*. [[CrossRef](#)]
28. Swift, B.J.F.; Baneyx, F. Microbial Uptake, Toxicity, and Fate of Biofabricated ZnS:Mn Nanocrystals. *PLoS ONE* **2015**, *10*, e0124916. [[CrossRef](#)] [[PubMed](#)]

29. Yang, Y.; Lv, S.-Y.; Yu, B.; Xu, S.; Shen, J.; Zhao, T.; Zhang, H. Hepatotoxicity assessment of Mn-doped ZnS quantum dots after repeated administration in mice. *Int. J. Nanomed.* **2015**, *10*, 5787–5796. [[CrossRef](#)] [[PubMed](#)]
30. Mohammad, F.; Al-Lohedan, H.A. Toxicity assessment of engineered Mn-ZnS quantum dots in vitro. *J. Mater. Sci.* **2016**, *51*, 9207–9216. [[CrossRef](#)]
31. Li, Y.; Zhang, H.; Guo, C.; Hu, G.; Wang, L. Multiresponsive Nanoprobes for Turn-On Fluorescence/19F MRI Dual-Modal Imaging. *Anal. Chem.* **2020**, *92*, 11739–11746. [[CrossRef](#)] [[PubMed](#)]
32. Pradhan, N.; Peng, X.G. Efficient and color-tunable Mn-doped ZnSe nanocrystal emitters: Control of optical performance via greener synthetic chemistry. *J. Am. Chem. Soc.* **2007**, *129*, 3339–3347. [[CrossRef](#)] [[PubMed](#)]
33. Xu, J.; Fan, Q.; Mahajan, K.D.; Ruan, G.; Herrington, A.; Tehrani, K.F.; Kner, P.; Winter, J.O. Micelle-templated composite quantum dots for super-resolution imaging. *Nanotechnology* **2014**, *25*, 195601. [[CrossRef](#)] [[PubMed](#)]
34. Dubertret, B.; Skourides, P.; Norris, D.J.; Noireaux, V.; Brivanlou, A.H.; Libchaber, A. In vivo imaging of quantum dots encapsulated in phospholipid micelles. *Science* **2002**, *298*, 1759–1762. [[CrossRef](#)]
35. Smith, W.E.; Brownell, J.; White, C.C.; Afsharnejad, Z.; Tsai, J.; Hu, X.; Polyak, S.J.; Gao, X.; Kavanagh, T.J.; Eaton, D.L. In Vitro Toxicity Assessment of Amphiphilic Polymer-Coated CdSe/ZnS Quantum Dots in Two Human Liver Cell Models. *ACS Nano* **2012**, *6*, 9475–9484. [[CrossRef](#)]
36. Liu, J.; Hu, R.; Liu, J.; Zhang, B.; Wang, Y.; Liu, X.; Law, W.C.; Liu, L.; Ye, L.; Yong, K.T. Cytotoxicity assessment of functionalized CdSe, CdTe and InP quantum dots in two human cancer cell models. *Mater. Sci. Eng. C Mater. Biol. Appl.* **2015**, *57*, 222–231. [[CrossRef](#)] [[PubMed](#)]
37. Wang, Y.; Tang, M. Review of in vitro toxicological research of quantum dot and potentially involved mechanisms. *Sci. Total Environ.* **2018**, *625*, 940–962. [[CrossRef](#)] [[PubMed](#)]
38. Pandey, V.; Pandey, G.; Tripathi, V.K.; Yadav, S.; Mudiam, M.K.R. Nucleation temperature-controlled synthesis and in vitro toxicity evaluation of l-cysteine-capped Mn:ZnS quantum dots for intracellular imaging. *Luminescence* **2016**, *31*, 341–347. [[CrossRef](#)]
39. Yang, Y.; Lv, S.; Wang, F.; An, Y.; Fang, N.; Zhang, W.; Zhao, W.; Guo, X.; Ji, S. Toxicity and serum metabolomics investigation of Mn-doped ZnS quantum dots in mice. *Int. J. Nanomed.* **2019**, *14*, 6297–6311. [[CrossRef](#)] [[PubMed](#)]
40. Labiadh, H.; Sellami, B.; Khazri, A.; Saidani, W.; Khemais, S. Optical properties and toxicity of undoped and Mn-doped ZnS semiconductor nanoparticles synthesized through the aqueous route. *Opt. Mater.* **2017**, *64*, 179–186. [[CrossRef](#)]
41. Popescu, T.; Matei, C.O.; Vlaicu, I.D.; Tivig, I.; Kuncser, A.C.; Stefan, M.; Ghica, D.; Miclea, L.C.; Savopol, T.; Culita, D.C.; et al. Influence of surfactant-tailored Mn-doped ZnO nanoparticles on ROS production and DNA damage induced in murine fibroblast cells. *Sci. Rep.* **2020**, *10*, 18062. [[CrossRef](#)]
42. Gaceur, M.; Giraud, M.; Hemadi, M.; Nowak, S.; Menguy, N.; Quisefit, J.P.; David, K.; Jahanbin, T.; Benderbous, S.; Boissière, M.; et al. Polyol-synthesized Zn_{0.9}Mn_{0.1}S nanoparticles as potential luminescent and magnetic bimodal imaging probes: Synthesis, characterization, and toxicity study. *J. Nanopart. Res.* **2012**, *14*, 932. [[CrossRef](#)]
43. Kuznetsova, V.A.; Vishratina, A.K.; Ryan, A.; Martynenko, I.V.; Loudon, A.; Maguire, C.M.; Purcell-Milton, F.; Orlova, A.O.; Baranov, A.V.; Fedorov, A.V.; et al. Enantioselective cytotoxicity of ZnS:Mn quantum dots in A549 cells. *Chirality* **2017**, *29*, 403–408. [[CrossRef](#)] [[PubMed](#)]
44. Selvaraj, J.; Mahesh, A.; Asokan, V.; Baskaralingam, V.; Dhayalan, A.; Paramasivam, T. Phosphine-Free, Highly Emissive, Water-Soluble Mn:ZnSe/ZnS Core-Shell Nanorods: Synthesis, Characterization, and in Vitro Bioimaging of HEK293 and HeLa Cells. *ACS Appl. Nano Mater.* **2018**, *1*, 371–383. [[CrossRef](#)]
45. Bae, J.; Lawrence, J.; Miesch, C.; Ribbe, A.; Li, W.; Emrick, T.; Zhu, J.; Hayward, R.C. Multifunctional Nanoparticle-Loaded Spherical and Wormlike Micelles Formed by Interfacial Instabilities. *Adv. Mater.* **2012**, *24*, 2735–2741. [[CrossRef](#)]
46. Duong, A.D.; Ruan, G.; Mahajan, K.; Winter, J.O.; Wyslouzil, B.E. Scalable, Semicontinuous Production of Micelles Encapsulating Nanoparticles via Electrospray. *Langmuir* **2014**, *30*, 3939–3948. [[CrossRef](#)] [[PubMed](#)]
47. Eugene, M. Polyethyleneglycols and immunocamouflage of the cells tissues and organs for transplantation. *Cell. Mol. Biol. (Noisy-Le-Grand)* **2004**, *50*, 209–215.
48. Hoshino, A.; Fujioka, K.; Oku, T.; Suga, M.; Sasaki, Y.F.; Ohta, T.; Yasuhara, M.; Suzuki, K.; Yamamoto, K. Physicochemical properties and cellular toxicity of nanocrystal quantum dots depend on their surface modification. *Nano Lett.* **2004**, *4*, 2163–2169. [[CrossRef](#)]
49. Tsoi, K.M.; Dai, Q.; Alman, B.A.; Chan, W.C.W. Are Quantum Dots Toxic? Exploring the Discrepancy Between Cell Culture and Animal Studies. *Acc. Chem. Res.* **2013**, *46*, 662–671. [[CrossRef](#)] [[PubMed](#)]
50. Porter, T. Development of Quantum Dots as Biosensing Probes. Bachelor's Thesis, The Ohio State University, Columbus, OH, USA, 2020.
51. Pradhan, N.; Battaglia, D.M.; Liu, Y.C.; Peng, X.G. Efficient, stable, small, and water-soluble doped ZnSe nanocrystal emitters as non-cadmium biomedical labels. *Nano Lett.* **2007**, *7*, 312–317. [[CrossRef](#)]
52. Zhu, J.; Hayward, R.C. Spontaneous generation of amphiphilic block copolymer micelles with multiple morphologies through interfacial instabilities. *J. Am. Chem. Soc.* **2008**, *130*, 7496–7502. [[CrossRef](#)]
53. Fan, Q. Designing Photo-Switchable Quantum Dots for Super Resolution Imaging. Ph.D. Thesis, OhioLINK Electronic Theses and Dissertations Center, The Ohio State University, Columbus, OH, USA, 2015.
54. Zhang, Y.; Clapp, A. Overview of Stabilizing Ligands for Biocompatible Quantum Dot Nanocrystals. *Sensors* **2011**, *11*, 11036–11055. [[CrossRef](#)] [[PubMed](#)]

55. Zhao, C.Z.; Bai, Z.L.; Liu, X.Y.; Zhang, Y.J.; Zou, B.S.; Zhong, H.Z. Small GSH-Capped CuInS₂ Quantum Dots: MPA-Assisted Aqueous Phase Transfer and Bioimaging Applications. *ACS Appl. Mater. Interfaces* **2015**, *7*, 17623–17629. [[CrossRef](#)]
56. Yong, K.T.; Law, W.C.; Hu, R.; Ye, L.; Liu, L.W.; Swihart, M.T.; Prasad, P.N. Nanotoxicity assessment of quantum dots: From cellular to primate studies. *Chem. Soc. Rev.* **2013**, *42*, 1236–1250. [[CrossRef](#)] [[PubMed](#)]
57. Salin, K.; Auer, S.K.; Rudolf, A.M.; Anderson, G.J.; Cairns, A.G.; Mullen, W.; Hartley, R.C.; Selman, C.; Metcalfe, N.B. Individuals with higher metabolic rates have lower levels of reactive oxygen species in vivo. *Biol. Lett.* **2015**, *11*. [[CrossRef](#)] [[PubMed](#)]
58. Lovric, J.; Cho, S.J.; Winnik, F.M.; Maysinger, D. Unmodified cadmium telluride quantum dots induce reactive oxygen species formation leading to multiple organelle damage and cell death. *Chem. Biol.* **2005**, *12*, 1227–1234. [[CrossRef](#)] [[PubMed](#)]
59. Ipe, B.I.; Lehnig, M.; Niemeyer, C.M. On the generation of free radical species from quantum dots. *Small* **2005**, *1*, 706–709. [[CrossRef](#)] [[PubMed](#)]
60. Wang, C.; Gao, X.; Su, X. Study the damage of DNA molecules induced by three kinds of aqueous nanoparticles. *Talanta* **2010**, *80*, 1228–1233. [[CrossRef](#)]
61. Anderson, N.C.; Hendricks, M.P.; Choi, J.J.; Owen, J.S. Ligand Exchange and the Stoichiometry of Metal Chalcogenide Nanocrystals: Spectroscopic Observation of Facile Metal-Carboxylate Displacement and Binding. *J. Am. Chem. Soc.* **2013**, *135*, 18536–18548. [[CrossRef](#)]
62. Shen, Y.; Tan, R.; Gee, M.Y.; Greytak, A.B. Quantum Yield Regeneration: Influence of Neutral Ligand Binding on Photophysical Properties in Colloidal Core/Shell Quantum Dots. *ACS Nano* **2015**, *9*, 3345–3359. [[CrossRef](#)]
63. Zhao, J.; Stenzel, M.H. Entry of nanoparticles into cells: The importance of nanoparticle properties. *Polym. Chem.* **2018**, *9*, 259–272. [[CrossRef](#)]